ARTICLE NO. 78-1307R

Modular, Spin-Stabilized, Tandem Solid Rocket Upper Stage

G. Porcelli* and E. Vogel†
Fairchild Space and Electronics Company, Germantown, Md.

This paper describes the main characteristics and the expected and postflight performance of a modular, spin-stabilized, tandem solid rocket upper stage. The stage provides the velocity increment required to supplement the inertial velocity attained by a launch vehicle for the injection of a payload into a prescribed orbit. Both an earlier design of the stage, in a single rocket configuration, and the current tandem design have been flight tested, the former in the course of the USAF Space Test Program P73-3, the latter during the launch of the first five satellites of the GPS (Global Positioning System) Phase I program. The modular approach to the tandem stage design provides a wide range of propulsion capability, since many combinations of existing solid rocket motors are possible. The stage has been flown and is currently being built for use with Atlas-F launch vehicles, but its design is compatible with other launch vehicles (Thor/Delta, Atlas SLV-3) and the Shuttle. Advantages of the spin-stabilized stage, compared to guided stages of the same class, are simplicity, ruggedness, reliability, and weight efficiency. This paper describes the basic design criteria, the main stage subsystems and components, and the expected performance. Postflight performance data from the P73-3 and the GPS programs are also presented.

Introduction

THE solid rocket upper stage (SRUS) is designed to provide: 1) a spin-stabilized attitude and 2) the velocity increment (ΔV) required to supplement the inertial velocity attained by a launch vehicle (LV) for the injection of a payload (spacecraft) into a prescribed orbit (ranging from circular low-altitude to synchronous transfer and escape orbits). The velocity increment is obtained by the burn of one or two solid rocket motors (SRM's) usable in many combinations. SRM's dimensionally compatible with the SRUS are those of the series Thiokol TE-M-364-2, -3, and -4, but other motors of smaller diameter are usable by the addition of a simple motor adapter ring. The large variety of SRM combinations offers a wide range of propulsion capabilities, as illustrated in a later section.

The SRUS is essentially composed of one or two SRM's combined in a modular assembly, the spin subsystem, the separation subsystem made up of spring/marman clamp assemblies providing the required number of separations, the power and electronic boxes, and the modular structure which provides mounting support and mechanical interface with the LV and the payload.

The SRUS performs the following functions: 1) SRUS/LV separation, 2) SRUS/payload spin-up, 3) first-stage ignition, 4) spent-stage separation, 5) second-stage ignition, 6) optional SRUS/payload despin (partial or total), and 7) SRUS/payload separation. These functions are sequenced by redundant electromechanical timers and associated circuitry.

The injection attitude is established by the LV prior to separation from the SRUS and maintained thereafter by means of spin stabilization initiated 0.3 s after separation to minimize LV induced attitude error buildup. For Shuttle applications with an electrically driven spin table, the spin subsystem is not required. Disturbances which contribute to orbit injection errors are: 1) The LV hand-off errors of altitude, velocity vector magnitude and angle (path and azimuth angles), attitude and angular rates (transverse axes), 2) the separation angular rates, 3) the attitude offset and nutation generated by spin system tolerances, 4) the average attitude offset and nutation during each SRM burn, due to motor thrust offset and angularity, motor mounting tolerances, and stage/payload center of mass (c.m.) tolerance, 5) the SRM impulse tolerances, 6) the SRM ignition timing errors, and 7) the attitude disturbance of the second stage caused by first-stage separation.

The SRUS design minimizes the effects of independent disturbances (such as the LV hand-off errors and the SRM errors) by proper selection of the separation and spin-up timing, and by proper choice of the spin rate based on a rational design of the spin subsystem. A description of SRUS design criteria, configuration, and subsystems, of performance prediction (payload capability and orbit injection accuracy), and of postflight performance data is contained in the following sections.

Basic SRUS Design

The SRUS design is illustrated in Fig. 1. The SRUS is basically composed of three segments called stages 0, 1 and 2, respectively. Stage 0 is only an interface structure with the LV. Stage 1 and stage 2 carry the SRM's and stage 2 is mated to the payload adapter structure. For a single-motor SRUS, the modular design permits replacement of the upper portion of the stage 1 structure with the payload adapter, thus eliminating stage 2, as Fig. 2 illustrates. The three separation subsystems, one on top of each stage, are composed of marman clamps and springs. The first subsystem provides separation of the SRUS from the LV, with which stage 0 remains. The second separation is activated to release the spent first stage. The third separation frees the payload from the spent second stage. The firing of the first SRM is controlled by redundant timers located in stage 1 and initiated at LV/SRUS separation. These timers also initiate stage 1/stage 2 separation. Sequencing of a second set of redundant timers, located in stage 2, is initiated at stage 1/stage 2 separation. These timers control the firing of the second SRM and the stage 2/payload separation.

The timing of the second separation is established on the basis of required minimum distance between the jettisoned stage 1 and the second stage at the time of second SRM

Presented as Paper 78-1307 at the AIAA Guidance and Control Conference, Palo Alto, Calif., Aug. 7-9, 1978; submitted Aug. 25, 1978; revision received Dec. 26, 1978.

Index categories: LV/M Dynamics and Control; Launch Vehicle Systems.

*Mgr., Dynamics and Control; presently, Sec. Chief, Spacecraft R&D, International Telecommunications Satellite Organization. Member AIAA.

†Principal Systems Design Eng., Dynamics and Control Section.

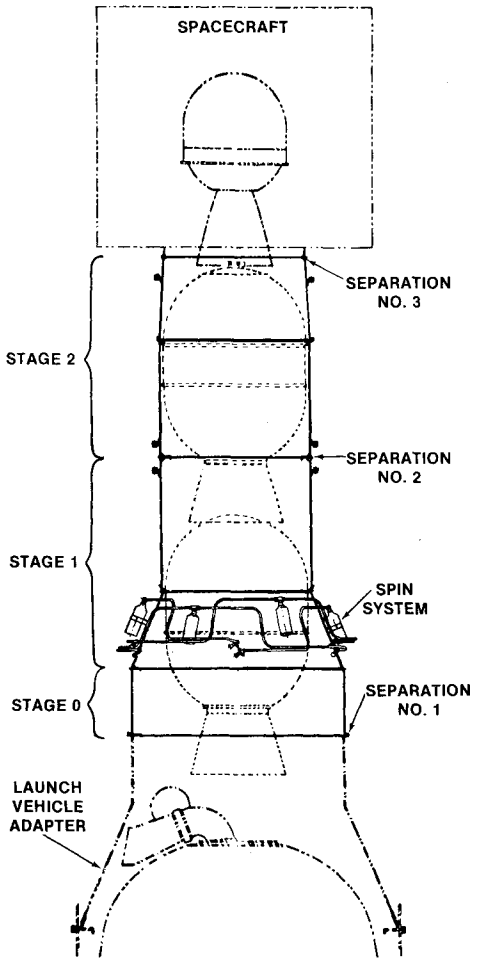

Fig. 1 Tandem SRUS configuration.

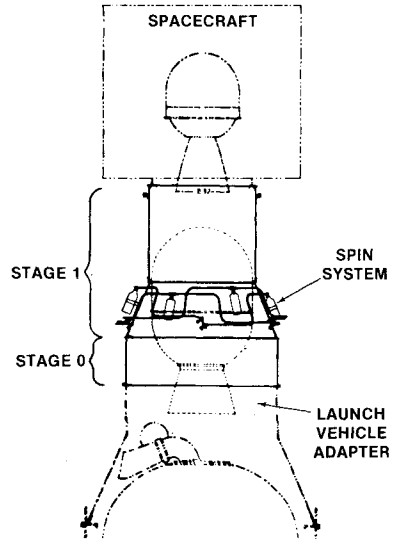

Fig. 2 Single-stage SRUS.

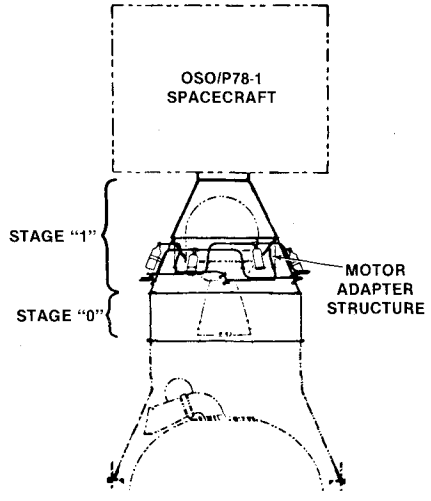

Fig. 3 SRUS for P78-1 program.

ignition, this distance being affected by the thrust "tail-off" characteristic of the first SRM and by the time difference between second separation and second ignition. Similarly, considerations of thrust tail-off and risk of recontact between the jettisoned second stage and the payload determine the timing of the third separation. Figure 3 illustrates the configuration of a single-stage SRUS to supply apogee insertion and orbit circularization for the SAMSO STP P78-1 program. This stage will provide both functions of spin-up and spin-down. Weight breakdowns of the P73, GPS, and P78 stage vehicles are given in Table 1. A view of a proposed tandem stage for perigee/apogee injection of a Shuttle-launched 1980 mission[1] is shown in Fig. 4. The figure also shows the airborne support equipment.

Spin Stabilization Subsystem

The spin subsystem, schematically illustrated in Figs. 1-3, is composed of a number of dual-nozzle hot-gas generators (HGG's). Each HGG is manifolded to a nozzle pair by equal length lines and the nozzles are mounted 180 deg apart on a transverse section of stage 1, with their thrust axis canted a certain angle aft from the transverse plane. The cant angle depends on the mass properties of the SRUS/payload, on the spin rate required, and on the number and impulse characteristics of the HGG's. Unique features of this design are:

1) Capability of varying the design spin rate by simply varying the nozzle cant angle.

2) Availability of an axial component of the total spin system impulse to provide additional SRUS/LV separation velocity.

3) A balanced torque couple is produced by each HGG, thus insuring a fail-safe spin system operation in case of one or more HGG failures.

Basic mechanical and impulse characteristics of the HGG's for the P73-3 and for the current GPS and P78-1 programs are illustrated in Fig. 5. Typical elements of the spin subsystems for the three programs are given in Table 2. The spin-up event, of the order of 0.3 s after SRUS separation from the LV, is initiated by a time-delay circuit.

The SRUS has the capability of partial or total despin before payload separation, by adding a despin system of HGG's on the last SRUS stage. For a single-stage SRUS, the despin system can be an integral part of the spin system, as in the P78-1 program.

Propulsion Subsystem

The main propulsion of the SRUS is provided by one or two SRM's. An SRM is essentially composed of a case containing the solid propellant, a nozzle, and an initiator. Typically, an SRM for upper-stage applications burns in a time span of 30-100 s; thus, for preliminary evaluations its performance can be assumed as impulsive. With appropriate fabrication and assembly controls, typical alignment tolerances normally guaranteed by manufacturers are: thrust/centerline offset = 0.25 mm (0.01 in.) and thrust/centerline angle = 0.002 rad. The total delivered impulse is also tightly controlled by accurate propellant casting and curing processes. Typical, guaranteed impulse tolerance is 0.75%. Because of their simplicity, SRM reliability figures are very high (normally greater than 0.999). The ratio of propellant weight to total

Table 1 Stage vehicle weight breakdown, kg

Program	P73	GPS	P78-1
Stage 0	61.7	61.7	56.7
Stage 1 structures	74.4	131.7	140.4
Stage 1 motor	1121.6[a]	1121.6[a]	362.6[b]
Stage 2 structures	...	74.1	...
Stage 2 motor	...	1121.6[a]	...
Total weight	1257.7	2510.7	559.7
Satellite weight	529	775	925

[a] TE-M-364-4.
[b] TE-M-616.

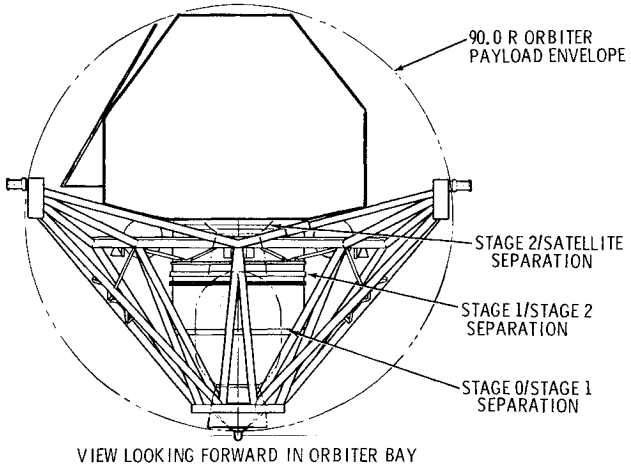

Fig. 4 View of SRUS for shuttle application.

motor weight (mass fraction) is normally of the order of 90% or higher. The specific impulse ranges between 285 and 300 lb-s/lb. Maximum motor diameter used in the presently configured SRUS is 37 in., which corresponds to that of the Thiokol Star 37 series. Motors of smaller diameter are accommodated by a conical adapter ring, as shown in Fig. 3.

The selection of the number (1 or 2) and size of each SRM depends on the impulse required to attain the necessary velocity increment and/or plane change, as required by the mission. Nominal mission requirements for the P73-3, the GPS, and the P78-1 missions are presented in Table 3.

A tandem-stage motor, Thiokol TE-M-364-4, is used for the GPS program. A single-stage TE-M-364-4 was flown in the P73-3 mission. A single-stage TE-M-616 is used in the P78-1 mission. Typical performance capability of the SRUS with different single and tandem combinations of the TE-M-364-3 and -4 motors is illustrated by the payload vs velocity increment curves of Fig. 6. These curves are suitable for preliminary planning.

Dynamic Performance

The dynamic performance of the SRUS mainly concerns its capability for maintaining a stable attitude and bounded nutation during SRM burns. A detailed presentation of the attitude and nutation error analysis goes beyond the scope of this paper. An indication of the performance attainable with a single-stage and a tandem SRUS is given by the results predicted in Tables 4 and 5, which also list typical event times. These results were obtained by application of classical mechanics.[2,3] The tables give the total attitude offsets; i.e., the combined pitch and yaw offset calculated at each event of the SRUS mission, and the corresponding event timings. The following significant elements are noted:

1) The attitude error contribution from all the sources of disturbance during SRUS performance is smaller than that originating from the launch vehicle hand-off errors. (Only the hand-off attitude errors contribute to angular errors, as listed in Tables 4 and 5.)

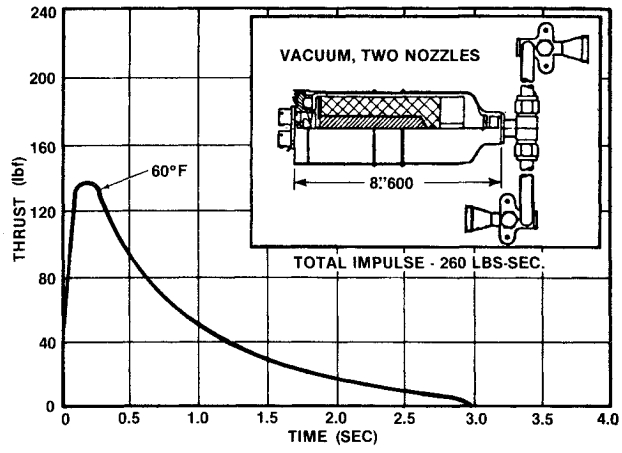

Fig. 5 HGG characteristics.

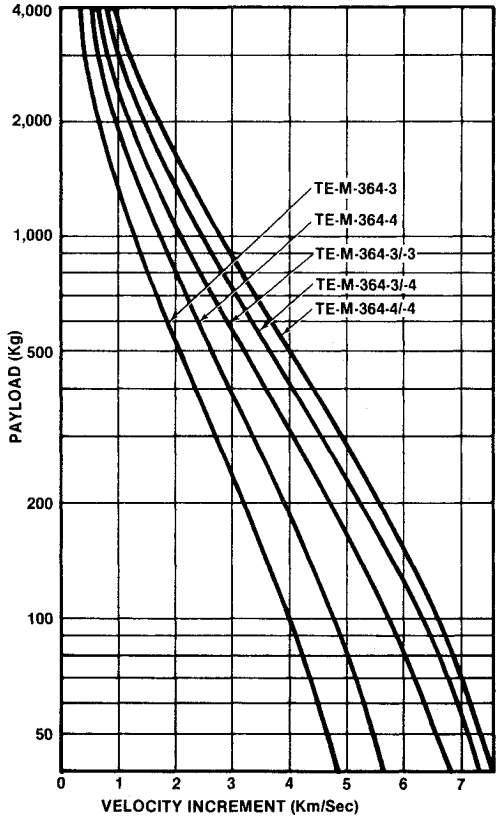

Fig. 6 Payload vs velocity increment.

2) By proper selection of the spin system ignition timing, the effects of the tip-off rates can be made negligible.

3) Although the SRUS is dynamically unstable ($I_s/I_t < 1$) until payload separation, and the payload carries an uncaged nutation damper, the effect of damper detuning during the phases preceding payload separation makes the dissipative component of nutation half-cone angle negligible with respect to that of rigid-body dynamics.

4) The significant increase of the spin/transverse moment-of-inertia ratio following each separation accounts for the corresponding sudden decrease of the nutation angle.

A sensitivity analysis of the effects of spin rate variation on attitude and nutation shows that at 75 rpm the 3σ cumulative attitude error at payload separation is 4.90 deg and the nutation half-cone angle is 1.20 deg (GPS).

The following represent the essential criteria imposed on the SRUS design by mission performance requirements: 1) at no time during the SRUS mission should the spin/transverse moment-of-inertia ratio approach 1; 2) coasting periods

Table 2 Spin subsystem

Program:	P73-3	GPS	P78-1	
Function	spin-up	spin-up	spin-up	spin-down
Number of HGG bottles	4	6	4	2
Total number of thrusters	8	12	8	4
Impulse per HGG bottle, N-s	1157	1157	1157	1157
Nozzle radius from spin axis, cm	56.6	75.56	76.55	76.55
Axial cant angle, deg	30	39.67	59.25	59.25
Radial cant angle, deg	19	0	0	0
Nominal spin rate, rpm	92.2	87.6	53.5	28.5
Axial ΔV, m/s	1.27	1.39	2.85	1.89

Table 3 Nominal mission requirements

Program:	P73-3	GPS	P78-1
SRUS configuration	single stage	tandem stage	single stage
Launch vehicle	ATLAS F	ATLAS F	ATLAS F
SRUS function	PKM	PKM	AKM
LV hand-off condition			
Altitude, km	185	172	256
Inertial velocity, m/s	6980	6660	7190
Path angle, deg	0.0	0.0	8.14
Velocity increment			
1st SRM, m/s	2600	1100	787
2nd SRM, m/s	...	2140	...
Transfer orbit			
Per. alt., km	193	154	−1705
Ap. alt., km	13,901	20,185	592
Semimaj. axis, km	13,425	16,548	5822
Eccentricity	0.5105	0.6052	0.1973
Inclination, deg	125	63	97.73

Table 4 Attitude and nutation error prediction (P73-3 single stage)

Event	Time, s	3-σ error increment, deg	3-σ error cumulative, deg	3-σ nutation ½-cone angle, deg
Launch vehicle	...	2.38	2.38	...
LV/SRUS separation	0-0.17	0.06	2.38	...
Spin-up	0.3-3.2	1.26	2.69	0.60
SRM burn (During)	20-64	1.17	2.93	1.75
SRM burn (End)		2.18	3.46	3.33
Coast	64-320	0.0	3.46	3.33
Payload separation	320	2.53	4.29	0.85

Table 5 Attitude and nutation error prediction (GPS tandem stage)

Event	Time, s	3-σ error increment, deg	3-σ error cumulative, deg	3-σ nutation ½-cone angle, deg
Launch vehicle	...	2.38	2.38	...
LV/SRUS separation	0	0.01	2.38	...
Spin-up	0.3-3.4	0.69	2.48	0.52
SRM 1 burn (During)	17-61.5	0.8	2.61	0.80
SRM 1 burn (End)		1.05	2.81	1.35
Coast	61.5-99.5	0.0	2.81	1.36
Stage 1 separation	99.5	0.39	2.84	0.97
Coast	99.55-116.5	0.0	2.84	0.97
SRM 2 burn (During)	116.5-161	0.95	2.99	1.20
SRM 2 burn (End)		1.48	3.34	2.42
Coast	161-416.5	0.0	3.34	2.87
Payload separation	416.56	1.99	3.88	0.88

Table 6 3-σ transfer orbit error prediction and postflight results (P73)

	Error effects		
	Apogee radius, km	Perigee radius, km	Inclination, deg
Mission requirements (3σ)	±900	...	±1.5
Preflight error estimates (3σ)	±348	±1.64	±0.56
Actual (postflight results)	−295	−1.0	+0.13

Table 7 3-σ transfer orbit error prediction and post flight results (GPS)

	Error effects		
	Apogee radius, km km	Perigee radius, km km	Inclination, deg
Mission requirements (3σ)	±520	± 6	±0.7
Preflight error estimates (3σ)	±346	±3.5	±0.47
Actual postflight results			
1st launch	−77	−1.5	+0.09
2nd launch	−211	+4.8	+0.1
3rd launch	−111	+1.67	+0.1
4th launch	−78	+1.8	−0.03
5th launch	−104	+0.1	+0.1

should be minimized, consistent with safe spin system and SRM ignition and payload separation, to minimize LV induced attitude error buildup and nutation buildup from energy dissipation sources in the payload (fuel slosh, uncaged dampers, etc.); 3) spin rate tradeoffs considering attitude/nutation error buildup and orbit insertion errors permit determination of minimum spin rate requirements.

Orbital Performance

A detailed presentation of the orbit error analysis exceeds the scope and limits of this paper. Fundamentals for this analysis are found in Refs. 3-5. Summaries of a covariance error analysis performed for the single-stage (P73-3) and for the tandem-stage (GPS) missions are given in Tables 6 and 7, respectively. These tables include the mission requirements and the effect of the following source errors (3σ):

1) Launch vehicle hand-off errors, provided by the LV supplier:

Altitude error	±250 m
Velocity	±2.6 mps
Flight path angle	±0.05 deg
Azimuth angle	±0.08 deg

with correlation coefficients all negligible, except

Altitude-velocity	−0.3
Altitude-path angle	−0.8
Velocity-path angle	+0.4

2) SRM impulse tolerances, as guaranteed by the supplier:

Impulse tolerance (at nominal temperature of 21 °C)	±0.75%
Impulse variation vs grain temperature variation	0.0087%/°C
Temperature variation	±8.3°C

3) Attitude errors during motor burn, as predicted in Tables 4 and 5.

4) Timer errors: ±1 s and ±4 s, respectively, for first and second stage.

The results of the analysis of the P73-3 and GPS flight telemetry data, given in Tables 6 and 7, show that actual performance was within the predicted 3σ error limits.

Conclusions

The design elements of a spin-stabilized, tandem solid rocket upper stage have been presented together with its expected dynamics and orbital performance. The postflight reduced data of this and of an earlier single-rocket version of the stage, also presented in the paper, demonstrated satisfactory performance. Main characteristics of the design, both in tandem- or single-rocket configuration, are: 1) the modular approach, which maximizes simplicity, cost-effectiveness, and payload capability, and 2) a flexible, fail-proof, spin system composed of canted, dual-nozzle, hot-gas generators providing spin rate and additional stage/launch vehicle separation velocity, both adjustable within wide ranges.

References

[1] Spencer, T.M., Glickman, R., and Porcelli, G., "Changing Inclination for Shuttle Payload," Paper 77-218, XXVIII IAF Congress, Prague, Czechoslovakia, 1977.

[2] Goldstein, H., *Classical Mechanics,* Addison-Wesley, Reading, Mass., 1959.

[3] Kaplan, M.H., *Modern Spacecraft Dynamics and Control,* J. Wiley, New York, 1976.

[4] Jensen, J., Townsend, G., Kork, J., and Kraft, D., *Design Guide to Orbital Flight,* McGraw-Hill Book Co., New York, 1962.

[5] Porcelli, G., Vogel, E., "Two-Impulse Orbit Transfer Error Analysis via Co-Variance Matrix," Paper 79-0256, AIAA 17th Aerospace Sciences Meeting, New Orleans, La., Jan. 1979.